

Long-term and seasonal variation of open-surface water bodies in the Yellow River Basin during 1990–2020

Chentai Jiao  | Shuai Wang  | Shuang Song | Bojie Fu

State Key Laboratory of Earth Surface Processes and Resource Ecology, Faculty of Geographical Science, Beijing Normal University, Beijing, China

Correspondence

Shuai Wang, State Key Laboratory of Earth Surface Processes and Resource Ecology, Faculty of Geographical Science, Beijing Normal University No. 19, XinJieKouWai St., HaiDian District, Beijing 100875, China.
 Email: shuaiwang@bnu.edu.cn

Funding information

Bayannur Ecological Governance and Green Development Academician Expert Workstation, Grant/Award Number: YSZ2018-1; Fundamental Research Funds for the Central Universities; National Natural Science Foundation of China, Grant/Award Numbers: 42041007, U2243601; the Science and Technology Project of Inner Mongolia Autonomous Region, Grant/Award Number: NMKJXM202109

Abstract

Open-surface water bodies are essential terrestrial water sources and ecosystem service providers, and their evaluation is necessary for effective water management. In this study, 36 000 Landsat images of the Yellow River Basin (YRB) were collected, and a multiple index (Modified Normalized Difference Water Index, Normalized Difference Vegetation Index and Enhanced Vegetation Index, i.e. MNDWI, NDVI and EVI) method was used to identify open-surface water bodies in the flood and dry seasons during 1990–2020. Our results showed that during these 30 years, YRB surface waters were characterized by spatial and seasonal heterogeneities. The open-surface water coverage in the upper and middle reaches of the YRB was 8.74% and 4.24%, respectively, less than the average coverage in the whole YRB of 9.45%. Surface water area was significant larger in flood seasons than in dry seasons, while during 1990–2020, the surface water area increased by 27.5% in the flood season and by 58.9% in the dry season, reaching 7239.2 km² (flood season) and 6654.8 km² (dry season) in 2020. Meanwhile the seasonal variation has decreased. Climate factors (winter temperature and summer precipitation) positively correlated with open-surface water only in the source region of the YRB. In other regions, anthropic factors (e.g. water conservation projects) strongly affected open-surface water bodies by increasing their spatial area overall and decreasing seasonal differences in their coverage.

KEY WORDS

big data, remote sensing, river system features, surface water bodies, Yellow River Basin

1 | INTRODUCTION

Open-surface water bodies are water bodies such as rivers, lakes, ponds, and artificial reservoirs exposed at the earth's surface, excluding the ocean. Open-surface water bodies are significant water sources that provide ecosystem services such as water supply and regulation, waste treatment, and recreation (Chen et al., 2020; Costanza et al., 1997; Deng et al., 2019; Jiao et al., 2021; Wood et al., 2011). However, climate change and anthropogenic activities have caused intensive global water changes that have led to spatial and temporal variations in open-surface water bodies (Chen et al., 2019; Cooley et al., 2021; Dai, 2013; Deng et al., 2019; Immerzeel et al., 2010; Milly et al., 2005; Pekel et al., 2016). For

example, in China, 90 000 km² of previously permanent water bodies vanished during 1984–2015 (Deng et al., 2019; Pekel et al., 2016), and water body areas in 10 midwestern states in the United States have been decreasing since 1984 (Zou et al., 2018). Changes in open-surface water bodies have led to increased pressure on water resources, especially in an arid and semi-arid areas. Therefore, monitoring open-surface water bodies is crucial for ensuring water supplies and achieving sustainable development.

The Yellow River (YR) is the fifth longest river in the world and the second longest river in China. The Yellow River Basin (YRB) supports a population of more than 100 million and provides 1/3 of China's grain yield but is limited by a shortage of water resources because of its location in an arid to semi-arid area (Fu et al., 2021; Xu

et al., 2005). The average runoff volume of the YRB accounts for only 2% of China's surface water, and it is characterized by a heterogeneous spatial distribution and significant temporal changes. Stream flow in the YRB estuary has significantly decreased since 1950s and keep steady in recent years. At the Lijin gauging station, the water discharge near the YRB estuary is about $175.20 \times 10^8 \text{ m}^3 \text{ year}^{-1}$ since the 2010s (Wang et al., 2019). This is approximately equal to the value of $195.94 \times 10^8 \text{ m}^3 \text{ year}^{-1}$ measured at Tangnaihai in the source region. To understand what has happened from the source region to the estuary, we need an accurate quantitative analysis of water bodies over long time series. Owing to the present and future water shortage in the YRB, effective water regulation and allocation schemes that rely on accurate and objective knowledge of water resources and supply are needed (Ringler et al., 2010). Therefore, monitoring of open-surface water bodies in the YRB should provide a foundation for environmental protection of the basin and its sustainable development.

Remote sensing is an effective method for accurately and efficiently extracting information on open-surface water bodies on a large spatial scale and over a long time period (Wang & Qin, 2018). Work and Gilmer (1976) extracted information on surface waters by supervised classification. McFeeters (1996) and Gao (1996) developed an early remote sensing water index—the Normalized Difference Water Index (NDWI)—from which the Modified Normalized Difference Water Index (MNDWI) was derived (Gao, 1996; McFeeters, 1996; Wang & Qin, 2018; Xu, 2005). These indices have been widely used for surface water monitoring research globally (Ding et al., 2017; Dzinotizei et al., 2018; Gu et al., 2007). However, threshold selection and the elimination of non-water dark pixels in these early remote sensing water indices usually involves considerable uncertainty. To overcome this problem, multiple remote sensing indices have recently been adopted for open-surface water body extraction. For example, Wu et al. (2018) developed the Two Steps Urban Water Index (TSUWI), and Zou et al. (2017, 2018) used the Enhanced Vegetation Index (EVI) and the NDVI in combination with the MNDWI to monitor open-surface water bodies in the contiguous United States (Wu et al., 2018; Zou et al., 2017, 2018). These updated methods improve the accuracy of water body extraction.

Multiple remote sensing datasets have been utilized in open-surface water extraction, where the Landsat TM/ETM+/OLI collection was preferred because of its long time series, medium to high resolution, acceptable revisit frequency and convenient data acquiring and processing (Deng et al., 2019; Pan et al., 2020; Zou et al., 2018). The spatial and temporal scales of most studies using traditional remote sensing water extraction methods have been limited by local data storage capacity and processing ability. Large data volume, intensive data processing requirements, and low calculation efficiency cause difficulties for researchers in large-scale and long-term research (Xia et al., 2022). The Google Earth Engine (GEE) platform provides an efficient solution for analysis of remote sensing big data. By accessing and processing remote sensing data on this cloud-based platform, the efficiency of geospatial data analysis can be significantly increased (Gorelick et al., 2017). However, relatively few studies have analysed open-surface water bodies in the YRB, and most have focused on only

a specific part of the basin or a specific period rather than on global and long-term features of open-surface water bodies (Li et al., 2017; Wang, Xia, et al., 2020; Wang, Xiao, et al., 2020; Zhou et al., 2021). Furthermore, most previous studies have defined permanent and seasonal water bodies based on water inundation frequency (Deng et al., 2019; Zhang et al., 2022), and the accurate identification of water bodies in different seasons has hardly been addressed. Yet intensive hydrological variation between seasons and possible trends of hydrological patterns in a certain season is upon concretize, making it important to understand exact features of open-surface water bodies in each season. Use of the GEE platform to obtain long time series of multiple indices at large spatial scale and the identification of seasonal open-surface water bodies can improve the understanding of open-surface water bodies in the YRB.

This study used the GEE platform, Landsat series images, and the MNDWI, NDVI, and EVI indices to monitor open-surface water bodies in the YRB and to show their seasonal variation during 1990–2020, when the YR was recovering after a dry period. Then, we analysed the results in combination with hydrological data to determine the factors influencing open-surface water bodies in the YRB. This study thus produces an accurate, quantified accounting of seasonal open-surface water bodies that can be used to improve water resource protection and regional sustainable development in the context of the rapid socio-economic growth of the YRB.

2 | DATA AND METHODS

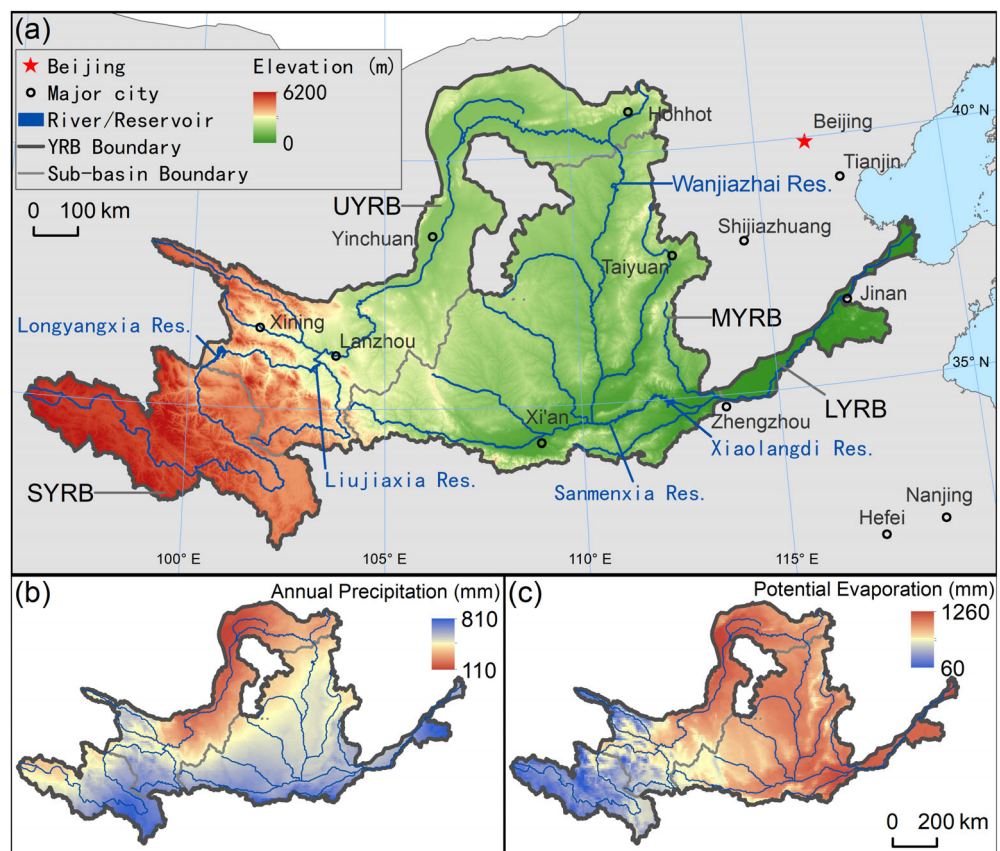
2.1 | Study area

The YR/YRB in northern China is $5.4 \times 10^3 \text{ km}$ long and covers $7.66 \times 10^5 \text{ km}^2$ ($95^{\circ}52'37''$ – $119^{\circ}3'56''$ E, $32^{\circ}9'38''$ – $41^{\circ}51'37''$ N), making it the second longest river and the second largest basin in China (Figure 1; Ringler et al., 2010). The river flows through nine provinces, as well as geomorphic areas including the Qinghai-Tibetan Plateau, the Loess Plateau, and the North China Plain. The river basin divided into four parts or sub-basins—Source, Upper, Middle and Lower (SYR/SYRB, UYR/UYRB, MYR/MYRB and LYR/LYRB, respectively). The YRB has a temperate continental-monsoon climate; the average annual temperature is 6.4°C , average annual precipitation is less than 500 mm, and annual potential evaporation is more than 800 mm (Liu et al., 2008; Xu et al., 2005). Thus, most of the YRB is in arid or semi-arid area (Figure 1). Furthermore, the distribution of natural water resources in the YRB is extremely uneven. In the MYRB and areas upstream, 85% of the total annual precipitation falls in summer (Wang et al., 2007), and 60% of the water contributed by the basin above Lanzhou (Hu & Zhang, 2018).

2.2 | Data

The landsat surface reflectance (SR) collection 1 was used after atmospheric correction by the LEDAPS and LaSRC algorithms. Landsat 5 Thematic Mapper images for 1990–2011 and Landsat 8 Operational

FIGURE 1 Study area.
 (a) Map of the Yellow River Basin (YRB). Sub-basins: SYRB, source YRB; UYRB, upper YRB; MYRB, middle YRB; LYRB, lower YRB.
 (b) Distributions of annual precipitation in the YRB.
 (c) Distributions of potential evaporation in the YRB.



Land Imager images for 2013–2020 were acquired from the GEE platform (Schmidt et al., 2013). In all, 36 078 images were used in this study. The images were evenly distributed both spatially and temporally (Figure 2). In addition, the Shuttle Radar Topography Mission Digital Elevation model (SRTM-DEM) from NASA, which has a horizontal resolution of 30 m and a vertical resolution of 1 m, was used (Farr et al., 2007). River network data were obtained from the Hydro-RIVERS database, which was produced by using SRTM-DEM data (Lehner et al., 2008; Lehner & Grill, 2013). The Joint Research Centre (JRC) global surface water database was used for masking non-water areas (Pekel et al., 2016). In addition, historical precipitation data from the TerraClimate dataset and historical temperature data from the ERA5 reanalysis dataset were acquired from the GEE platform, and historical monthly discharge data were obtained from the Yellow River Conservancy Commission (Abatzoglou et al., 2018; Hersbach et al., 2020; Li et al., 2021).

2.3 | Methods

2.3.1 | Pre-processing of remote sensing data

Landsat SR data were first radiometrically calibrated and atmospherically corrected. Then, the F-mask method was used to mask cloud, shadow, and ice+snow pixels (Zhu & Woodcock, 2012). To reduce the error introduced by selection of images from different dates over

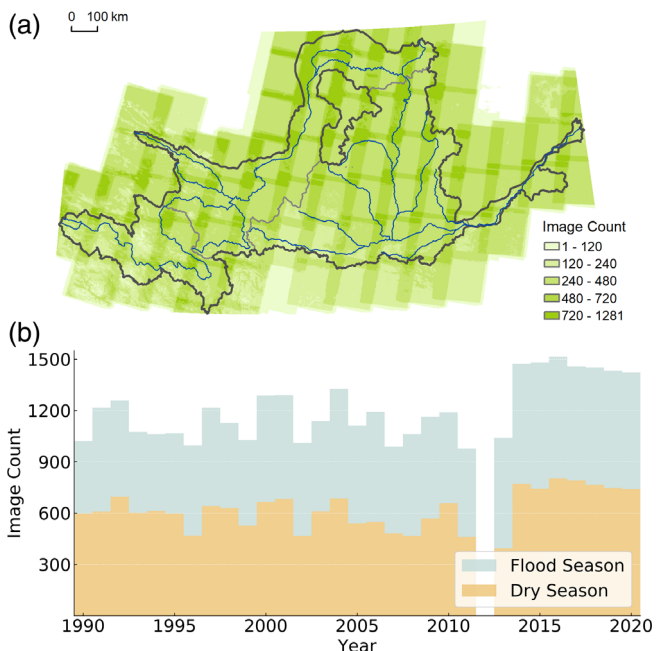


FIGURE 2 (a) Spatial and (b) temporal distributions of Landsat images.

30 years, the GEE-provided median function was used to produce an integrated image of the YRB in each season and year. Figure 3 provides a flowchart of the study.

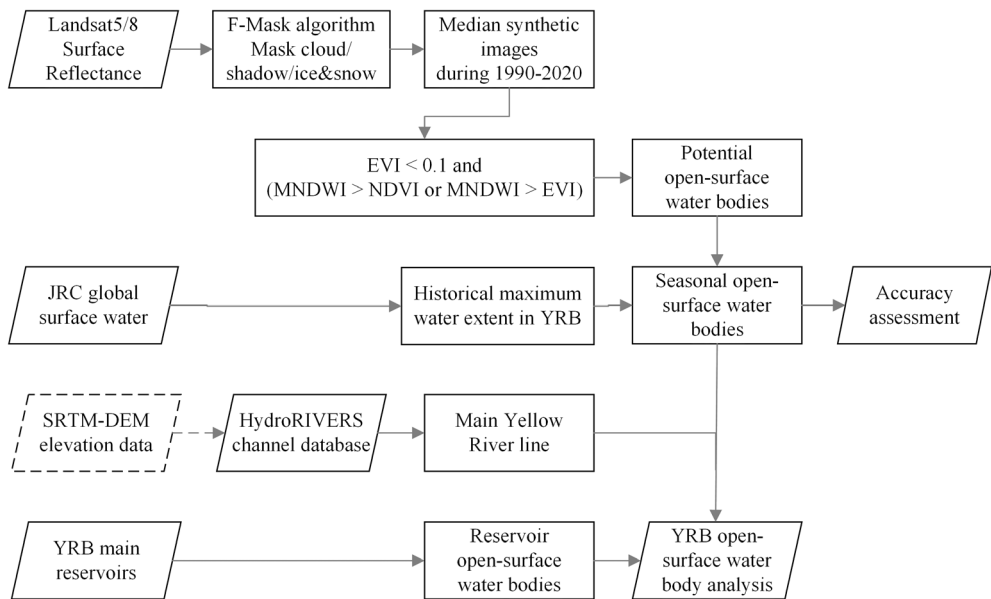


FIGURE 3 Flowchart of study procedures.

2.3.2 | Water extraction algorithms

Three indices, MNDWI, NDVI, and EVI, were used to extract open-surface water bodies in the YRB (Figure 3; Deng et al., 2019; Zou et al., 2018). The indices were calculated as follows:

$$\text{MNDWI} = \frac{G - \text{SWIR}}{G + \text{SWIR}} \quad (1)$$

$$\text{NDVI} = \frac{\text{NIR} - R}{\text{NIR} + R} \quad (2)$$

$$\text{EVI} = \frac{2.5 \times (\text{NIR} - R)}{\text{NIR} + 6 \times R - 7.5 \times B + 1} \quad (3)$$

where B, G, R, NIR, and SWIR refer to the blue, green, red, near-infrared, and short-wave infrared (short-wave infrared 1 for Landsat 8) bands of the Landsat SR images. In each year, the 6 months from May to October were considered the flood season, and the other months were considered the dry season. MNDWI was calculated using the seasonal median integrated image, whereas EVI and NDVI were calculated using the annual median combined image to reduce the influence of phenology. After these calculations, the rules proposed by Zou et al. (2018) were adopted to define the water pixels (Zou et al., 2018). If the output of the following Boolean operation was yes, the pixel was defined as a potential water pixel.

$$\text{if } [\text{EVI} < 0.1 \text{ and } (\text{MNDWI} > \text{NDVI} \text{ or } \text{MNDWI} > \text{EVI})] \quad (4)$$

Compared to traditionally used methods such as manual threshold selection or Otsu's method, multi-index water extraction reduces spatial incompatibility resulting from use of a single threshold in the complex YRB and increases extraction accuracy.

Occurrence data from the JRC Global Surface Water Database were used to generate a mask (Pekel et al., 2016). A potential water pixel was defined as water only if the output of the following Boolean operation was yes.

$$\text{if } (\text{Occurrence} > 0) \quad (5)$$

This mask was introduced to further reduce disturbance from snow or shadows and to increase the extraction accuracy (Deng et al., 2019; Sidjak, 1999).

Three indices: water frequency, open-surface water coverage and F/D ratio are defined based on extracted open-surfaces water bodies. Water frequency is defined as the occurrence number of open-surfaces water bodies in a pixel during the 30 flood seasons and 30 dry seasons from 1990 to 2020, and expressed as a fraction with a denominator of 60. Open-surface water coverage refers to the proportion covered by open-surfaces water bodies in a certain area. F/D ratio is defined as the ratio between the open-surface water extents of flood season and dry season in a year. These indices are used for spatial and temporal analyses on open-surface water bodies.

2.3.3 | Accuracy assessment

Water extraction accuracy was evaluated by visual interpretation. A 90-m-wide buffer area was created outside the extracted water area with a size approximately equal to the water area and defined as a non-water area. Next, 2000 accuracy assessment points were created by the equalized stratified random method. Then a confusion matrix was constructed based on visual interpretation of the Landsat true colour synthetic SR image (Table 1). The result showed that the overall water extraction accuracy was 92.80% with a kappa coefficient of 0.856. This level of accuracy was considered acceptable for further analysis.

2.3.4 | Extraction of reservoir water bodies and river width

Five major reservoirs on the main YR (Longyangxia Reservoir, Liujiashia Reservoir, Wanjiashai Reservoir, Sanmenxia Reservoir and Xiaolangdi Reservoir, according to the Yellow River Conservancy Commission) were included in the water body analysis. The surface water extent of each reservoir water body was determined by defining the water

surface altitude at the dam as the lower limit, and the water level at the upstream boundary as the upper limit. The 30-year maximum water extent was generated based on the water bodies extracted in each season by remote sensing.

The width of the mainstream of the YR was calculated by using both remote-sensing-extracted and HydroRIVERS data. First, the first-level river line within the YRB was selected as the centre line of the mainstream. Next, water bodies within 3.5 km of the centre line

TABLE 1 The confusion matrix used for accuracy assessment.

Classification	Landsat SR image			User's accuracy
	Water	Non-water	Total	
Water	947	53	1000	94.70%
Non-water	91	909	1000	90.90%
Total	1038	962	2000	Overall accuracy = 92.80%
Producer's accuracy	91.23%	94.49%		Kappa coefficient = 0.856

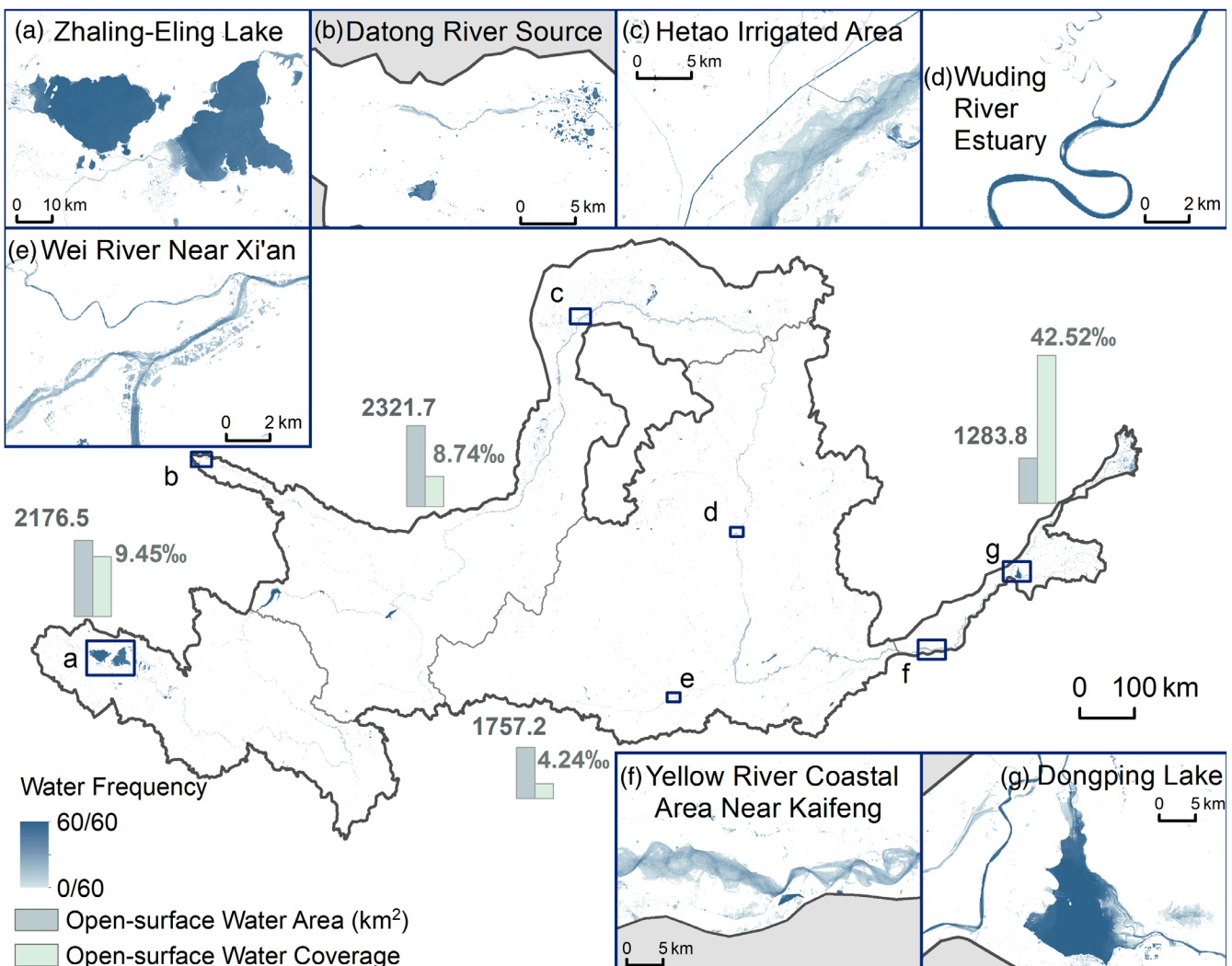


FIGURE 4 Spatial distribution of open-surface water bodies in each YRB sub-basins and selected subareas (1990–2020): (a) Zhaling-Eling Lake, (b) Datong River source, (c) Hetao irrigated area, (d) Wuding River estuary, (e) Wei River near Xi'an, (f) Yellow River coastal area near Kaifeng, and (g) Dongping Lake.

were defined as main river water bodies and extracted with a buffer and overlay analysis. The width of the mainstream was defined as the ratio of the area of the main river water bodies and the length of the first-level river line.

3 | RESULTS

3.1 | Spatial pattern

Open-surface water bodies in the YRB showed strong spatial heterogeneity (Figure 4). During the 2020 flood season, the total area of open-surface water bodies in the YRB was 7239.2 km², the highest extent since 1990, and accounted for 9.45% of the total area of the basin. In the SYRB, the open-surface water body area was 2176.5 km²; most of these water bodies were in the Zhaling-Eling lake area. Open-surface water bodies in the UYRB occupied an area of 2321.7 km² and accounted for 32.1% of the total area of open-surface water bodies in the YRB, but the open-surface water coverage was only 8.74%, below the average for the YRB. The open-surface water body area in the MYRB was 1757.2 km²; the open-surface water coverage was 4.24%, only 44.9% of the average ratio in the YRB. The open-surface water body area in the LYRB was smallest among the four sub-basins (1283.8 km² or 17.7% of the total open-surface water body area in the YRB). However, the open-surface water coverage was 42.52%, the highest in the YRB. The five essential reservoirs covered a total area of 626.9 km² and together

accounted for 9.48% of the total open-surface water body area in the YRB (Figure S1).

The mean width of the YR also varied spatially (Figure 5). During the 2020 flood season, the mean width was 0.535 km. The SYR had the largest width of 0.581 km, followed by the LYR (0.561 km wide), the MYR (0.490 km), and the UYR (0.456 km). In the 2020 dry season, the mean width of the YR was 0.452 km. The mean widths of the SYR, LYR, UYR, and MYR were 0.501, 0.460, 0.419, and 0.389 km, respectively.

3.2 | Seasonal variation

Open-surface water bodies in the YRB showed distinct variations between flood and dry seasons. More open-surface water bodies were identified during flood seasons (Figure 6). The open-surface water body area showed a moderately significant difference ($BF_{10} \geq 3$) between the flood and dry season in the MYRB and an extremely significant difference ($BF_{10} \geq 100$) in the other three sub-basins and in the whole YRB (Bayesian t-test, 30 sample pairs each test). In addition, the mean width of the whole YR and the river width in all four sub-basins showed extremely significant seasonal differences ($BF_{10} \geq 100$) during 1990–2020 (Bayesian t-test, 30 sample pairs each test) (Figure 5). However, the F/D ratio decreased during the study period, and the decreasing trend was significant ($p < 0.01$). In 2014 and 2017, the surface water extent of open-surface water bodies was greater in the dry seasons than in the flood seasons (Figure 6).

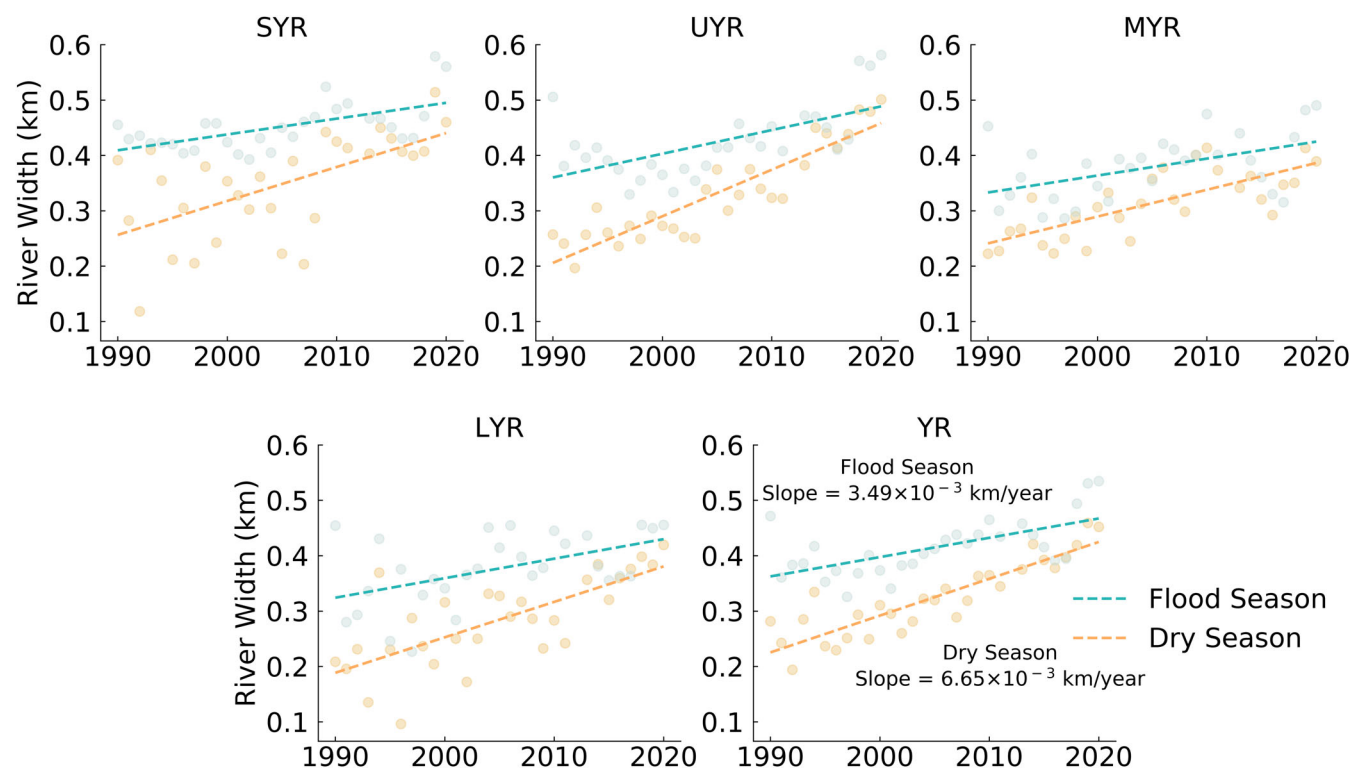


FIGURE 5 Interannual trends in the mean width of the Yellow River and its four parts. (SYR, source YR; UYR, upper YR; MYR, middle YR; LYR, lower YR.)

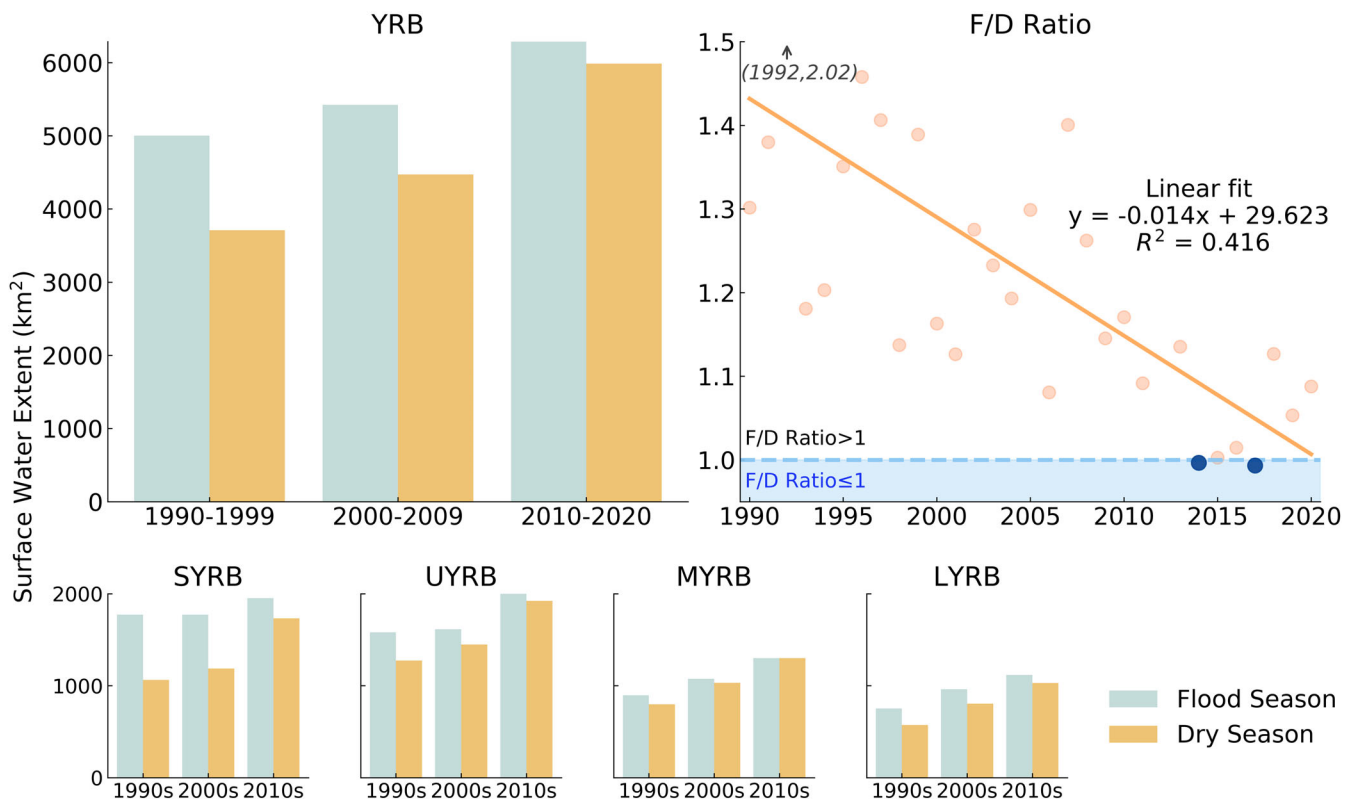


FIGURE 6 Seasonal surface water extent in the YRB and its sub-basins, and the change in the flood season/dry season ratio (F/D ratio) from 1990 to 2020.

The seasonal features of the five major reservoirs differed from those of other open-surface water bodies in the whole YRB. Four of the reservoirs (excepting Longyangxia Reservoir) had larger water surface areas in the dry season than in the flood season. The F/D ratios of Wanjiashan Reservoir and Sanmenxia Reservoir decreased from 1.00 and 1.08, respectively, in the 1990s, to 0.90 and 0.81, respectively, in the 2010s. The recently built Xiaolangdi Reservoir experienced dramatic changes during 1999–2003. During this period, its surface water area increased by 36.6 km^2 per year, and it was transformed from an elongated channel-shaped water body to a broad reservoir with an F/D ratio consistently less than 1 (Figure S2).

3.3 | Time series trends

The surface water extent of the open-surface water bodies in the YRB showed an increasing trend during the 30-year study period (Figure 7). In flood seasons, the surface water extent increased steadily from 5002.2 km^2 in the 1990s to 6376.8 km^2 in the 2010s, on average, for a percentage increase of 27.5%. In dry seasons, the surface water extent of water bodies fluctuated among years, but showed a rapid increase from 3372.2 km^2 in the 1990s to 5356.9 km^2 in the 2010s, on average, for a percentage increase of 58.9%. Likewise, the surface area extents of open-surface water bodies in each of the four sub-basins of the YRB increased by 10.1%–79.5% during the study period. In all sub-basins, the surface water extent of open-

surface water bodies increased at a higher rate in the dry season than in the flood season. The mean width of the YR also increased from the 1990s to the 2010s, from 0.384 km to 0.456 km in the flood season and from 0.260 km to 0.400 km in the dry season (Figure 5).

4 | DISCUSSION

4.1 | Climate influences

Seasonal variations of open-surface water bodies in the YRB dominantly reflect climate features, especially precipitation patterns. During 1990–2020, the average annual precipitation in the YRB was 462 mm , 87% of which fell in flood seasons. The vast seasonal differences in rainfall led to an uneven water supply. Thus, the surface water extent of open-surface water bodies in the YRB also varied seasonally (Wang, Xia, et al., 2020; Wang, Xiao, et al., 2020). Climate change is a potential factor influencing open-surface water bodies in the YRB. Precipitation and temperature have been shown to significantly influence the discharge of the YR (Li et al., 2019; Xu, 2007; Yan et al., 2020; Zhou et al., 2022). Our Bayesian correlation analysis showed that, in the SYRB, precipitation in flood seasons and temperature in dry seasons were strongly correlated with the surface water extent of open-surface water bodies in the YRB (30 sample pairs each test) (Figure S3). Furthermore, the SYR discharge at Tangnaihai gauge showed an extremely strong correlation ($\text{BF}_{10} \geq 100$) with the surface

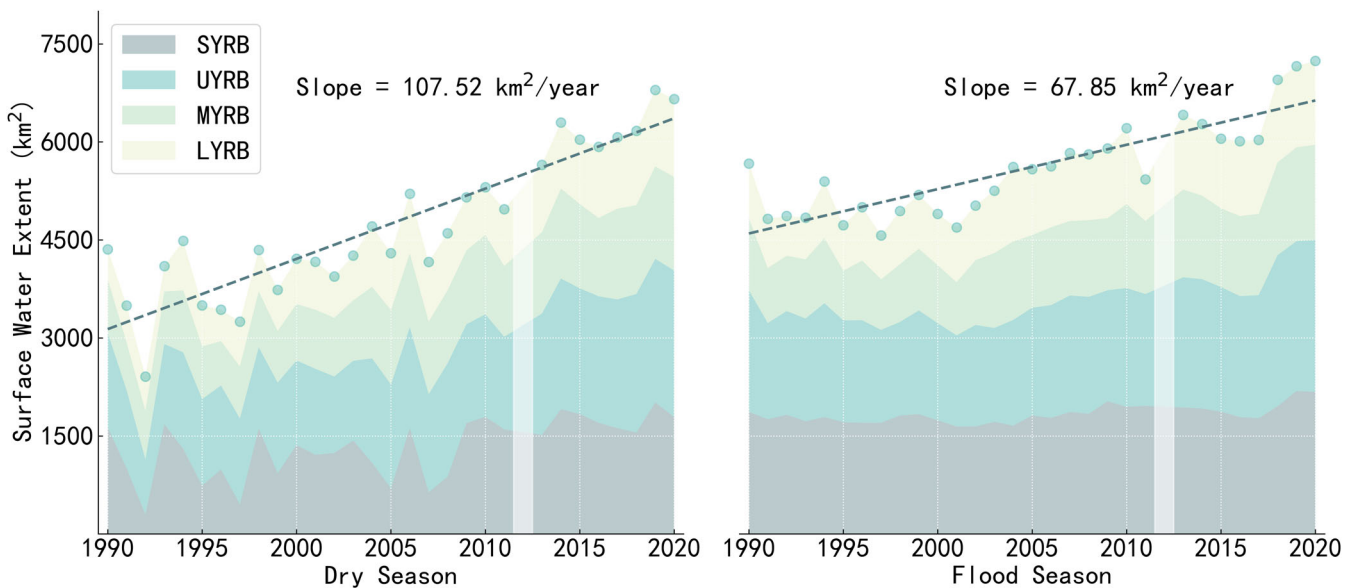


FIGURE 7 Interannual changes in the surface water extent of open-surface water bodies in the YRB during the dry season (left) and flood season (right) (1990–2020).

water extent of open-surface bodies in the SYRB (excluding reservoirs) in flood seasons and moderate correlation in dry seasons ($BF_{10} \geq 3$) (Bayesian correlation analysis, 30 sample pairs each test). These results suggest that temperature in winter and spring influences the amount of meltwater from glaciers and snow and contribute, along with precipitation, to the water supply to open-surface water bodies in the YRB in the flood seasons.

In contrast, in the other sub-basins, the correlations between temperature and precipitation with the surface water extents of open-surface water bodies were relatively weak (Figure S3). Thus, the relationship between climate features and open-surface water bodies was weaker downstream, where anthropogenic activity plays a more important role (Wang et al., 2018).

4.2 | Anthropogenic influences

Anthropogenic activity, represented by water conservation projects, also affects open-surface water bodies in the YRB. The five essential reservoirs have different seasonal features from natural water bodies; in particular, their F/D ratio is smaller than 1. Reservoirs such as Xiaolangdi Reservoir are operated so as to release water before the flood season begins and then to hold runoff during the flood season (Hu, 2016; Kong et al., 2022). In combination with other water conservation practices in the YRB, this mode of reservoir operation reduces flood peaks and increases water availability during the dry season, thus reducing the F/D ratio (Kong et al., 2022). Water conservation structures in the YRB have significantly changed hydrological processes and interannual trends. Gauge data and recent studies show that the discharge of the YR has been decreasing during the last 50 years; moreover, since 1998, water consumption has been increasing. Nevertheless, the surface water extent of open-surface water bodies and the width of the mainstream have increased (Yan

et al., 2013; Zhang et al., 2011). The Bayesian analysis results also show that the discharge and water body area are less correlated below the SYRB. These results are attributed to water management.

Not only do water conservation practices help to maintain a uniform discharge and prevent seasonal drying of rivers, artificial intervention has also increased the surface water extent of other types of water bodies. In particular, coastal and deltaic wetlands in the LYRB have increased in area, and construction of new reservoirs throughout the YRB has played an essential role in increasing open-surface water bodies in the YRB (Figure 8) (Zhang et al., 2021). Basin management and ecological restoration are effective in maintaining open-surface water bodies. As a response to the decreasing runoff, the artificially induced continuous increase of the surface water extent can be recognized as an adaption to hydrological drought during and after the 1990s (Shiau et al., 2007; Wang et al., 2023). The results indicates that surface waters have increased in time and space and have become more stable since 1990, thereby ensuring ecosystem services such as water supply and the regulation of disturbance.

While the increase in open-surface water bodies contributes to YRB's water resource availability, it should be noted that it may also have a negative effect on water resources. Droughts have been increasing in the YRB, and hydrological droughts are estimated to be more intense than meteorological droughts (Wang et al., 2023). Open-surface water bodies play a crucial role in altering the relationship between meteorological and hydrological droughts. The expansion of open-surface water bodies increases regional evaporation, leading to a decrease in surface water resources as well as soil and groundwater resources (Wang et al., 2023). Anthropogenic water management has reduced seasonal variation, thereby limiting the intensity of hydrological droughts, but it can only affect the allocation of water, not the overall amount (Wang et al., 2016). Therefore, the increase in water bodies may actually decrease the water resource amount in the YRB.

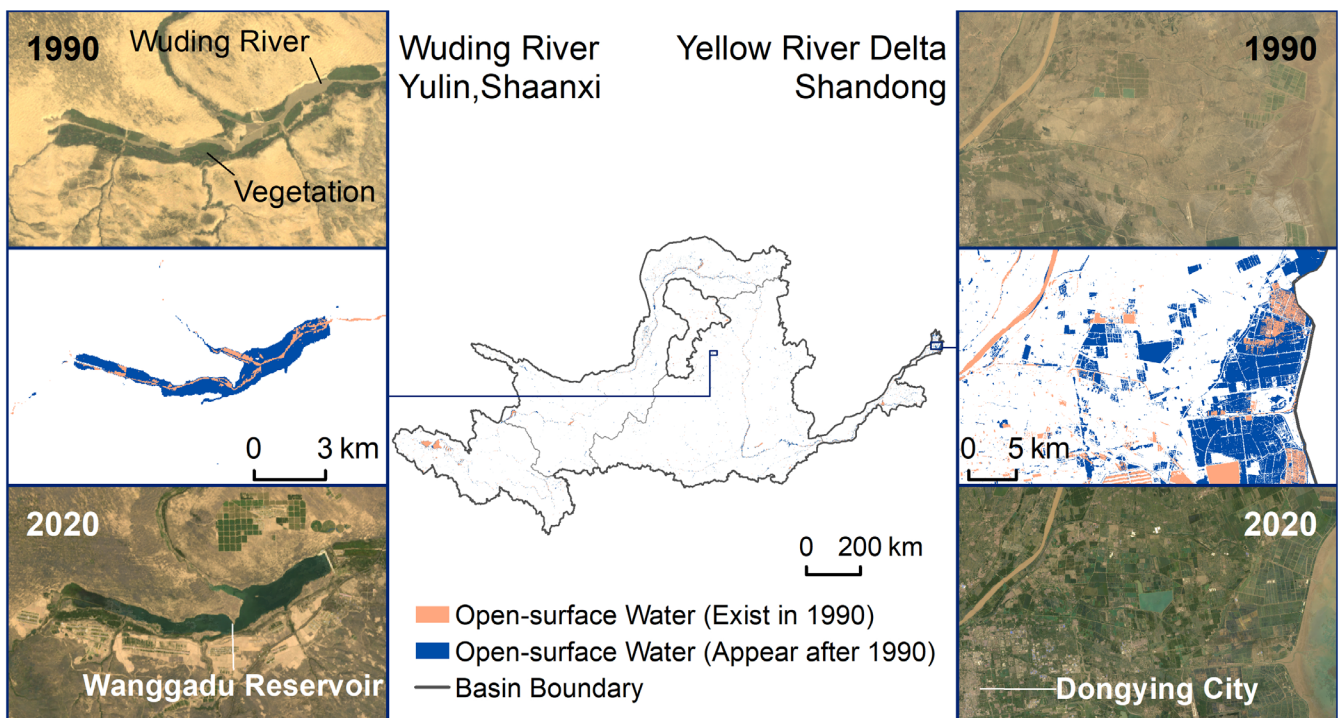


FIGURE 8 Examples of changes to open-surface water bodies in the YRB between 1990 and 2020.

4.3 | Uncertainty and limitations

Use of the GEE platform for water extraction in this study achieved good accuracy, but uncertainties remain. First, misclassification of ice or shadows as water bodies by the multiple indices used in this study limits the accuracy, and JRC data must be used to correct such misclassification. In addition, seasonal vegetation dynamics potentially influences indices such as the NDVI and EVI. To control for the resultant errors, NDVI and EVI data for wet and dry seasons were not evaluated separately in this study. Thus, the efficiency of water indices can still be improved. Second, this study extracted past open-surface water bodies in the YRB, but less attention was paid to the factors driving their distribution and their dynamics. Also, the investigations of future changes to open-surface water bodies are still needed.

5 | CONCLUSION

This study used the GEE platform, Landsat series images, and the MNDWI, NDVI and EVI to seasonally monitor open-surface water bodies in the YRB during 1990–2020. The results confirmed that open-surface water bodies in the YRB were unevenly distributed and the total area was lacking. Open-surface water coverage in the LYRB, the whole YRB and the MYRB were 42.52%, 9.45% and 4.24%, respectively, which indicates a strongly heterogeneous spatial distribution. In addition, open-surface water bodies in YRB showed distinct seasonal variability: both the total area of open-surface water bodies and the mean width of the YR showed significant differences between dry seasons and flood seasons.

Open-surface water bodies in the YRB and in each of its four sub-basins have increased in area in the last 30 years, as has the mean width of the YR. The rate of increase in the dry seasons was 214% that in the flood season. Climate change in the SYRB and anthropogenic activities throughout the YRB have strongly affected the open-surface water bodies in YRB. Water conservation practices such as reservoir construction, by increasing the total area of open-surface water bodies and decreasing seasonal variation, are effective adaptations to drought in the YRB.

ACKNOWLEDGEMENTS

This research was supported by the National Natural Science Foundation of China (grant no. 42041007 and U2243601), the ‘Fundamental Research Funds for the Central Universities’, Bayannur Ecological Governance and Green Development Academician Expert Workstation (YSZ2018-1), and the Science and Technology Project of Inner Mongolia Autonomous Region (NMKJXM202109).

DATA AVAILABILITY STATEMENT

Data used in this research include raster data, river network data and statistical data. Raster data include remote sensing images (Landsat TM and OLI), DEM data (SRTM-DEM), JRC global surface water database and climate reanalysis data (precipitation from TerraClimate dataset and temperature from the ERA5 reanalysis dataset). All raster data above were acquired through Google Earth Engine platform (<https://earthengine.google.com/>). River network data are extracted from HydroRIVERS (Asia) dataset and can be downloaded from <https://www.hydroseds.org/products/hydrorivers>. Statistical data used is monthly discharge data of the Yellow River from the Yellow

River Conservancy Commission, Ministry of Water Resources, China. This research has produced seasonal open-surface water body data in YRB during 1990–2020 (excluding 2012). These data are available upon request.

ORCID

Chentai Jiao  <https://orcid.org/0000-0003-1737-9814>

Shuai Wang  <https://orcid.org/0000-0003-1595-9858>

REFERENCES

- Abatzoglou, J. T., Dobrowski, S. Z., Parks, S. A., & Hegewisch, K. C. (2018). TerraClimate, a high-resolution global dataset of monthly climate and climatic water balance from 1958–2015. *Scientific Data*, 5(1), 170191. <https://doi.org/10.1038/sdata.2017.191>
- Chen, J., Kang, T., Yang, S., Bu, J., Cao, K., & Gao, Y. (2020). Open-surface water bodies dynamics analysis in the Tarim River basin (North-Western China), based on Google earth engine cloud platform. *Water*, 12(10), 2822. <https://doi.org/10.3390/w12102822>
- Chen, S. A., Michaelides, K., Grieve, S. W. D., & Singer, M. B. (2019). Aridity is expressed in river topography globally. *Nature*, 573(7775), 573–577. <https://doi.org/10.1038/s41586-019-1558-8>
- Cooley, S. W., Ryan, J. C., & Smith, L. C. (2021). Human alteration of global surface water storage variability. *Nature*, 591(7848), 78–81. <https://doi.org/10.1038/s41586-021-03262-3>
- Costanza, R., d'Arge, R., de Groot, R., Farber, S., Grasso, M., Hannon, B., Limburg, K., Naeem, S., O'Neill, R. V., Paruelo, J., Raskin, R. G., Sutton, P., & van den Belt, M. (1997). The value of the world's ecosystem services and natural capital. *Nature*, 387(6630), 253–260. <https://doi.org/10.1038/387253a0>
- Dai, A. (2013). Increasing drought under global warming in observations and models. *Nature Climate Change*, 3(1), 52–58. <https://doi.org/10.1038/nclimate1633>
- Deng, Y., Jiang, W., Tang, Z., Ling, Z., & Wu, Z. (2019). Long-term changes of open-surface water bodies in the Yangtze River basin based on the Google earth engine cloud platform. *Remote Sensing*, 11(19), 2213. <https://doi.org/10.3390/rs11192213>
- Ding, C., Liu, X., Huang, F., Li, Y., & Zou, X. (2017). Onset of drying and dormancy in relation to water dynamics of semi-arid grasslands from MODIS NDWI. *Agricultural and Forest Meteorology*, 234–235, 22–30. <https://doi.org/10.1016/j.agrformet.2016.12.006>
- Dzinotizei, Z., Murwira, A., Zengeya, F. M., & Guerrini, L. (2018). Mapping waterholes and testing for aridity using a remote sensing water index in a southern African semi-arid wildlife area. *Geocarto International*, 33(11), 1268–1280. <https://doi.org/10.1080/10106049.2017.1343394>
- Farr, T. G., Rosen, P. A., Caro, E., Crippen, R., Duren, R., Hensley, S., Kobrick, M., Paller, M., Rodriguez, E., Roth, L., Seal, D., Shaffer, S., Shimada, J., Umland, J., Werner, M., Oskin, M., Burbank, D., & Alsdorf, D. (2007). The shuttle radar topography mission. *Reviews of Geophysics*, 45(2), RG2004. <https://doi.org/10.1029/2005RG000183>
- Fu, B., Wang, S., Shen, Y., Cheng, C., Li, Y., Feng, X., & Liu, Y. (2021). Mechanisms of human–natural system coupling and optimization of the Yellow River Basin. *Bulletin of National Natural Science Foundation of China*, 35(4), 504–509. <https://doi.org/10.16262/j.cnki.1000-8217.2021.04.002>
- Gao, B. C. (1996). NDWI - a normalized difference water index for remote sensing of vegetation liquid water from space. *Remote Sensing of Environment*, 58(3), 257–266. [https://doi.org/10.1016/S0034-4257\(96\)00067-3](https://doi.org/10.1016/S0034-4257(96)00067-3)
- Gorelick, N., Hancher, M., Dixon, M., Ilyushchenko, S., Thau, D., & Moore, R. (2017). Google earth engine: Planetary-scale geospatial analysis for everyone. *Remote Sensing of Environment*, 202, 18–27. <https://doi.org/10.1016/j.rse.2017.06.031>
- Gu, Y., Brown, J. F., Verdin, J. P., & Wardlow, B. (2007). A five-year analysis of MODIS NDVI and NDWI for grassland drought assessment over the central Great Plains of the United States. *Geophysical Research Letters*, 34(6), L06407. <https://doi.org/10.1029/2006GL029127>
- Hersbach, H., Bell, B., Berrisford, P., Hirahara, S., Horányi, A., Muñoz-Sabater, J., Nicolas, J., Peubey, C., Radu, R., Schepers, D., Simmons, A., Soci, C., Abdalla, S., Abellan, X., Balsamo, G., Bechtold, P., Biavati, G., Bidlot, J., Bonavita, M., ... Thépaut, J.-N. (2020). The ERA5 global reanalysis. *Quarterly Journal of the Royal Meteorological Society*, 146(730), 1999–2049. <https://doi.org/10.1002/qj.3803>
- Hu, C. (2016). Development and practice of the operation mode of storing clear water and discharging muddy flow in sediment-laden rivers in China. *Journal of Hydraulic Engineering*, 47(3), 283–291.
- Hu, C., & Zhang, X. (2018). Several key questions in the researches of runoff and sediment changes and trend predictions in the Yellow River. *Journal of Hydraulic Engineering*, 49(9), 1028–1039.
- Immerzeel, W. W., van Beek, L. P. H., & Bierkens, M. F. P. (2010). Climate change will affect the Asian water towers. *Science*, 328(5984), 1382–1385. <https://doi.org/10.1126/science.1183188>
- Jiao, C., Song, S., Huang, Q., Xia, X., & Zhang, Y. (2021). Dynamics of open-surface water in Guanting reservoir basin: A Google earth engine platform study. *Journal of Beijing Normal University. Natural Science*, 57(5), 639–647. <https://doi.org/10.12202/j.0476-0301.2021084>
- Kong, D., Miao, C., Duan, Q., Li, J., Zheng, H., & Gou, J. (2022). Xiaolangdi dam: A valve for streamflow extremes on the lower Yellow River. *Journal of Hydrology*, 606, 127426. <https://doi.org/10.1016/j.jhydrol.2022.127426>
- Lehner, B., & Grill, G. (2013). Global river hydrography and network routing: Baseline data and new approaches to study the world's large river systems. *Hydrological Processes*, 27(15), 2171–2186. <https://doi.org/10.1002/hyp.9740>
- Lehner, B., Verdin, K., & Jarvis, A. (2008). New global hydrography derived from spaceborne elevation data. *Eos, Transactions American Geophysical Union*, 89(10), 93–94. <https://doi.org/10.1029/2008EO100001>
- Li, B., Mu, X., Gao, P., Zhao, G., & Sun, W. (2019). New characteristics of temporal and spatial changes of runoff in the mainstream of Yellow River from 1956 to 2017. *Research of Soil and Water Conservation*, 26(8), 120–126, 132.
- Li, C., Fu, B., Wang, S., Stringer, L. C., Wang, Y., Li, Z., Liu, Y., & Zhou, W. (2021). Drivers and impacts of changes in China's drylands. *Nature Reviews Earth & Environment*, 2(12), 858–873. <https://doi.org/10.1038/s43017-021-00226-z>
- Li, W., Wang, X., Li, T., Mao, W., & Yao, L. (2017). Extraction method of spectral information of inland surface water body in Yellow River Basin. *Bulletin of Soil and Water Conservation*, 37(2), 158–164.
- Liu, Q., Yang, Z., & Cui, B. (2008). Spatial and temporal variability of annual precipitation during 1961–2006 in Yellow River Basin, China. *Journal of Hydrology*, 361(3), 330–338. <https://doi.org/10.1016/j.jhydrol.2008.08.002>
- McFeeters, S. K. (1996). The use of the normalized difference water index (NDWI) in the delineation of open water features. *International Journal of Remote Sensing*, 17(7), 1425–1432. <https://doi.org/10.1080/01431169608948714>
- Milly, P. C. D., Dunne, K. A., & Vecchia, A. V. (2005). Global pattern of trends in streamflow and water availability in a changing climate. *Nature*, 438(7066), 347–350. <https://doi.org/10.1038/nature04312>
- Pan, F., Xi, X., & Wang, C. (2020). A comparative study of water indices and image classification algorithms for mapping inland surface water bodies using Landsat imagery. *Remote Sensing*, 12(10), 1611. <https://doi.org/10.3390/rs12101611>
- Pekel, J.-F., Cottam, A., Gorelick, N., & Belward, A. S. (2016). High-resolution mapping of global surface water and its long-term changes. *Nature*, 540(7633), 418–422. <https://doi.org/10.1038/nature20584>
- Ringler, C., Cai, X., Wang, J., Ahmed, A., Xue, Y., Xu, Z., Yang, E., Jianshi, Z., Zhu, T., Cheng, L., Yongfeng, F., Xinfeng, F., Xiaowei, G., & You, L.

- (2010). Yellow River basin: Living with scarcity. *Water International*, 35(5), 681–701. <https://doi.org/10.1080/02508060.2010.509857>
- Schmidt, G., Jenkerson, C., Masek, J., Vermote, E., & Gao, F. (2013). Landsat ecosystem disturbance adaptive processing system (LEDAPS) algorithm description (Open-File Report No. 2013-1057). U.S. Geological Survey. <https://pubs.usgs.gov/of/2013/1057/>
- Shiau, J.-T., Feng, S., & Nadarajah, S. (2007). Assessment of hydrological droughts for the Yellow River, China, using copulas. *Hydrological Processes*, 21(16), 2157–2163. <https://doi.org/10.1002/hyp.6400>
- Sidjak, R. W. (1999). Glacier mapping of the Illecillewaet icefield, British Columbia, Canada, using Landsat TM and digital elevation data. *International Journal of Remote Sensing*, 20(2), 273–284. <https://doi.org/10.1080/014311699213442>
- Wang, H., & Qin, F. (2018). Summary of the research on water body extraction and application from remote sensing image. *Science of Surveying and Mapping*, 43(5), 23–32. <https://doi.org/10.16262/j.cnki.1000-8217.2021.04.002>
- Wang, H., Yang, Z., Saito, Y., Liu, J. P., Sun, X., & Wang, Y. (2007). Stepwise decreases of the Huanghe (Yellow River) sediment load (1950–2005): Impacts of climate change and human activities. *Global and Planetary Change*, 57(3), 331–354. <https://doi.org/10.1016/j.gloplacha.2007.01.003>
- Wang, R., Xia, H., Qin, Y., Niu, W., Pan, L., Li, R., Zhao, X., Bian, X., & Fu, P. (2020). Dynamic monitoring of surface water area during 1989–2019 in the Hetao plain using Landsat data in Google earth engine. *Water*, 12(11), 3010. <https://doi.org/10.3390/w12113010>
- Wang, S., Fu, B., Piao, S., Lü, Y., Ciais, P., Feng, X., & Wang, Y. (2016). Reduced sediment transport in the Yellow River due to anthropogenic changes. *Nature Geoscience*, 9(1), 1–41. <https://doi.org/10.1038/ngeo2602>
- Wang, X., Engel, B., Yuan, X., & Yuan, P. (2018). Variation analysis of Streamflows from 1956 to 2016 along the Yellow River, China. *Water*, 10(9), 1231. <https://doi.org/10.3390/w10091231>
- Wang, X., Xiao, X., Zou, Z., Dong, J., Qin, Y., Doughty, R. B., Menarguez, M. A., Chen, B., Wang, J., Ye, H., Ma, J., Zhong, Q., Zhao, B., & Li, B. (2020). Gainers and losers of surface and terrestrial water resources in China during 1989–2016. *Nature Communications*, 11(1), 3471. <https://doi.org/10.1038/s41467-020-17103-w>
- Wang, Y., Wang, S., Chen, Y., Wang, F., Liu, Y., & Zhao, W. (2023). Anthropogenic drought in the Yellow River basin: Multifaceted and weakening connections between meteorological and hydrological droughts. *Journal of Hydrology*, 129273, 129273. <https://doi.org/10.1016/j.jhydrol.2023.129273>
- Wang, Y., Zhao, W., Wang, S., Feng, X., & Liu, Y. (2019). Yellow River water rebalanced by human regulation. *Scientific Reports*, 9(1), 9707.
- Wood, E. F., Roundy, J. K., Troy, T. J., van Beek, L. P. H., Bierkens, M. F. P., Blyth, E., de Roo, A., Döll, P., Ek, M., Famiglietti, J., Gochis, D., van de Giesen, N., Houser, P., Jaffé, P. R., Kollet, S., Lehner, B., Lettenmaier, D. P., Peters-Lidard, C., Sivapalan, M., ... Whitehead, P. (2011). Hyperresolution global land surface modeling: Meeting a grand challenge for monitoring Earth's terrestrial water. *Water Resources Research*, 47, W05301. <https://doi.org/10.1029/2010WR010090>
- Work, E., & Gilmer, D. (1976). Utilization of satellite data for inventorying prairie ponds and lakes. *Photogrammetric Engineering and Remote Sensing*, 42(5), 685–694.
- Wu, W., Li, Q., Zhang, Y., Du, X., & Wang, H. (2018). Two-step urban water index (TSUWI): A new technique for high-resolution mapping of urban surface water. *Remote Sensing*, 10(11), 1704. <https://doi.org/10.3390/rs10111704>
- Xia, X., Jiao, C., Song, S., Zhang, L., Feng, X., & Huang, Q. (2022). Developing a method for assessing environmental sustainability based on the Google earth engine platform. *Environmental Science and Pollution Research*, 29(38), 57437–57452. <https://doi.org/10.1007/s11356-022-19773-z>
- Xu, H. (2005). A study on information extraction of water body with the modified normalized difference water index (MNDWI). *Journal of Remote Sensing*, 9(5), 589–595.
- Xu, J. (2007). Impact of human activities on the stream flow of Yellow River. *Advances in Water Science*, 18(5), 648–655.
- Xu, Z. X., Takeuchi, K., Ishidaira, H., & Liu, C. M. (2005). An overview of water resources in the Yellow River basin. *Water International*, 30(2), 225–238. <https://doi.org/10.1080/02508060508691863>
- Yan, D., Lai, Z., & Ji, G. (2020). Using Budyko-type equations for separating the impacts of climate and vegetation change on runoff in the source area of the Yellow River. *Water*, 12(12), 3418. <https://doi.org/10.3390/w12123418>
- Yan, W., YongJian, D., BaiSheng, Y., FengJing, L., Jie, W., & Jie, W. (2013). Contributions of climate and human activities to changes in runoff of the yellow and Yangtze rivers from 1950 to 2008. *Science China Earth Sciences*, 56(8), 1398–1412. <https://doi.org/10.1007/s11430-012-4505-1>
- Zhang, Q., Singh, V. P., Sun, P., Chen, X., Zhang, Z., & Li, J. (2011). Precipitation and streamflow changes in China: Changing patterns, causes and implications. *Journal of Hydrology*, 410(3), 204–216. <https://doi.org/10.1016/j.jhydrol.2011.09.017>
- Zhang, X., Wang, G., Xue, B., Zhang, M., & Tan, Z. (2021). Dynamic landscapes and the driving forces in the Yellow River Delta wetland region in the past four decades. *Science of the Total Environment*, 787, 147644. <https://doi.org/10.1016/j.scitotenv.2021.147644>
- Zhang, Y., Du, J., Guo, L., Fang, S., Zhang, J., Sun, B., Mao, J., Sheng, Z., & Li, L. (2022). Long-term detection and spatiotemporal variation analysis of open-surface water bodies in the Yellow River Basin from 1986 to 2020. *Science of the Total Environment*, 845, 157152. <https://doi.org/10.1016/j.scitotenv.2022.157152>
- Zhou, H., Liu, S., Hu, S., & Mo, X. (2021). Retrieving dynamics of the surface water extent in the upper reach of Yellow River. *Science of the Total Environment*, 800, 149348. <https://doi.org/10.1016/j.scitotenv.2021.149348>
- Zhou, Z., Liu, J., Yan, Z., Wang, H., & Jia, Y. (2022). Attribution analysis of the natural runoff evolution in the Yellow River basin. *Advances in Water Science*, 33(1), 27–37.
- Zhu, Z., & Woodcock, C. E. (2012). Object-based cloud and cloud shadow detection in Landsat imagery. *Remote Sensing of Environment*, 118, 83–94. <https://doi.org/10.1016/j.rse.2011.10.028>
- Zou, Z., Dong, J., Menarguez, M. A., Xiao, X., Qin, Y., Doughty, R. B., Hooker, K. V., & David Hambright, K. (2017). Continued decrease of open surface water body area in Oklahoma during 1984–2015. *Science of the Total Environment*, 595, 451–460. <https://doi.org/10.1016/j.scitotenv.2017.03.259>
- Zou, Z., Xiao, X., Dong, J., Qin, Y., Doughty, R. B., Menarguez, M. A., Zhang, G., & Wang, J. (2018). Divergent trends of open-surface water body area in the contiguous United States from 1984 to 2016. *Proceedings of the National Academy of Sciences*, 115(15), 3810–3815. <https://doi.org/10.1073/pnas.1719275115>

SUPPORTING INFORMATION

Additional supporting information can be found online in the Supporting Information section at the end of this article.

How to cite this article: Jiao, C., Wang, S., Song, S., & Fu, B. (2023). Long-term and seasonal variation of open-surface water bodies in the Yellow River Basin during 1990–2020. *Hydrological Processes*, 37(3), e14846. <https://doi.org/10.1002/hyp.14846>